Bioorganic & Medicinal Chemistry xxx (xxxx) xxxx

Contents lists available at ScienceDirect

Bioorganic & Medicinal Chemistry

journal homepage: www.elsevier.com/locate/bmc

Synthesis, biological evaluation and anti-proliferative mechanism of fluorine-containing proguanil derivatives

Di Xiao[a], Zhicheng Lu[b], Zhiren Wang[a], Sichun Zhou[a], Mengru Cao[c], Jun Deng[a], Xin Hu[a], Mei Peng[a], Caimei He[a], Jingtao Wu[a], Simeng Xu[a], Huihui Zhang[a], Cangcang Xu[a], Wei Wang[c,*], Aiying Guan[b,*], Xiaoping Yang[a,*]

[a] Key Laboratory of Study and Discovery of Small Targeted Molecules of Hunan Province, Department of Pharmacy, School of Medicine, Hunan Normal University, Changsha, Hunan, China
[b] State Key Laboratory of the Discovery and Development of Novel Pesticide, Shenyang Sinochem Agrochemicals R&D Company Ltd., Shenyang, China
[c] TCM and Ethnomedicine Innovation & Development International Laboratory, Innovative Materia Medical Research Institute, School of Pharmacy, Hunan University of Chinese Medicine, Changsha, China

ARTICLE INFO

Keywords:
Biguanides
Fluorine-containing compounds
Anti-proliferative
AMPK

ABSTRACT

Proguanil, a member of biguanide family, has excellent anti-proliferative activities. Fluorine-containing compounds have been demonstrated to have super biological activities including enhanced binding interactions, metabolic stability, and reduced toxicity. In this study, based on the intermediate derivatization methods, we synthesized 13 new fluorine-containing proguanil derivatives, and found that **7a**,**7d** and **8e** had much lower IC_{50} than proguanil in 5 human cancerous cell lines. The results of clonogenic and scratch wound healing assays revealed that the inhibitory effects of derivatives **7a**,**7d** and **8e** on proliferation and migration of human cancer cell lines were much better than proguanil as well. Mechanistic study based on representative derivative **7a** indicated that this compound up-regulates AMPK signal pathway and downregulates mTOR/4EBP1/p70S6K. In conclusion, these new fluorine-containing derivatives show potential for the development of cancer chemotherapeutic drugs.

1. Introduction

Around the world, it is estimated that there were 9.6 million cancer deaths in 2018, and to search high efficacy and safe anti-proliferative drugs is still a tough challenge.[1] Biguanides have been used clinically to treat diabetes (metformin) or malaria (proguanil).[2–4] Interestingly, anti-proliferative activities of biguanide drugs, especially metformin have attracted considerable attention in recent years.[5,6] However, preclinical studies have shown that effective metformin concentration to kill cancer cells is always in the milli molar range, making it difficult to translate into clinical administration since it is practically arduous to achieve this high concentration via conventional administration routes.[7] In contrast, we noticed that proguanil (Fig.1), a member of the biguanide family, has been demonstrated to have excellent anti-proliferative effects. Lea et al reported that among the biguanides including buformin, phenformin, proguanil and phenyl biguanide, proguanil has the strongest inhibitory effect on nine cancer cell lines.[8] Based on the intermediate derivatization method, further chemical modifications to proguanil will have a great potential to obtain superior anti-proliferative compounds.[9]

Fluorine-containing compounds have been demonstrated to have super biological activities including enhanced binding interactions, metabolic stability, and reduced toxicity.[10–12] The introduction of fluorine into drugs has become common, and best-performing drugs on the present market contain fluorine atom.[13] Particularly, in the anti-tumor drug market, most of compounds, particularly targeted drugs including Gefitinib and Olaparib, have fluorine atom.[14,15] Previous studies in our laboratory have also demonstrated that fluorinated quercetin plays a better role in the treatment of bladder cancer than quercetin.[16] In present study, we introduced a fluorine or fluoroalkyl into a specific position of the biguanide backbone, and found that derivatives **7a**,**7d** and **8e** have a stronger inhibitory effect on the

Abbreviations: THF, Tetrahydrofuran; SAR, Structure activity relationship; HRMS, High resolution mass spectrometry; ESI, Electrospray ionization; HPLC, High-performance liquid chromatography; PBS, Phosphatebuffered saline; SDS-PAGE, Sodium dodecyl sulphate polyacrylamide gel electrophoresis; PVDF, Polyvinylidene fluoride; TBST, Tris-buffered saline with 0.1% Tween

* Corresponding authors.
E-mail addresses: wangwei402@hotmail.com (W. Wang), guanaiying@sinochem.com (A. Guan), xiaoping.yang@hunnu.edu.cn (X. Yang).

https://doi.org/10.1016/j.bmc.2019.115258
Received 22 August 2019; Received in revised form 28 November 2019; Accepted 7 December 2019

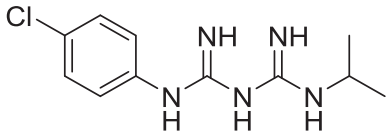

Fig. 1. Chemical structure of proguanil.

proliferation and invasive phenotype of cancer cells than proguanil.

2. Results and discussion

2.1. Chemistry

The target derivatives **7a-7f**,**8a-8e** and **9a-9b** were synthesized according to the method as shown in Scheme 1. The commercially available compounds 4-(trifluoromethyl) aniline, 4-fluoroaniline, 3,4-difluoroaniline, and 2,4-difluoroaniline were firstly reacted respectively with sodium dicyandiamide at 80 °C to obtain corresponding intermediates. They were then separately reacted with alkylamines or cycloalkylamines at 40 °C in tetrahydrofuran (THF) until the intermediate compounds were completely reacted. Finally, after HCl solution was added and stirred for 30 min, ammonia ethylenediaminetetraacetic acid (EDTA) solution was dripped to the reaction mixture and filtered to obtain the target derivatives **7a-7f**,**8a-8e** and **9a-9b**.[17,18]

2.2. In vitro inhibitory effect on cell proliferation of fluorine-containing derivatives

Anti-proliferative activity of these derivatives to human cancer cell lines were detected by 3-(4,5-dimethylthiazol-2-yl)-2,5-diphenyltetrazolium bromide (MTT) assay, as each compound's IC_{50} values illustrated in Table 1. Fig 2 illustrated the concentration-response curves for proguanil, **7a,7d** and **8e**. As shown in Table 1, most derivatives demonstrated significant anti-proliferative activity to these tested cancer cell lines, especially to lung cancer cell line A549. Furthermore, anti-proliferative effects of derivatives **7a**, **7d** and **8e** in all cancer cell lines were even greatly stronger than proguanil (Table 1 and Fig.2). Most interestingly, derivative **7a** showed best anti-proliferative activities with IC_{50} value of 2.0 μM for UMUC3, 3.1 μM for T24, 1.3 μM for A549 among 13 tested derivatives (Table 1). In contrast, anti-proliferative activity of

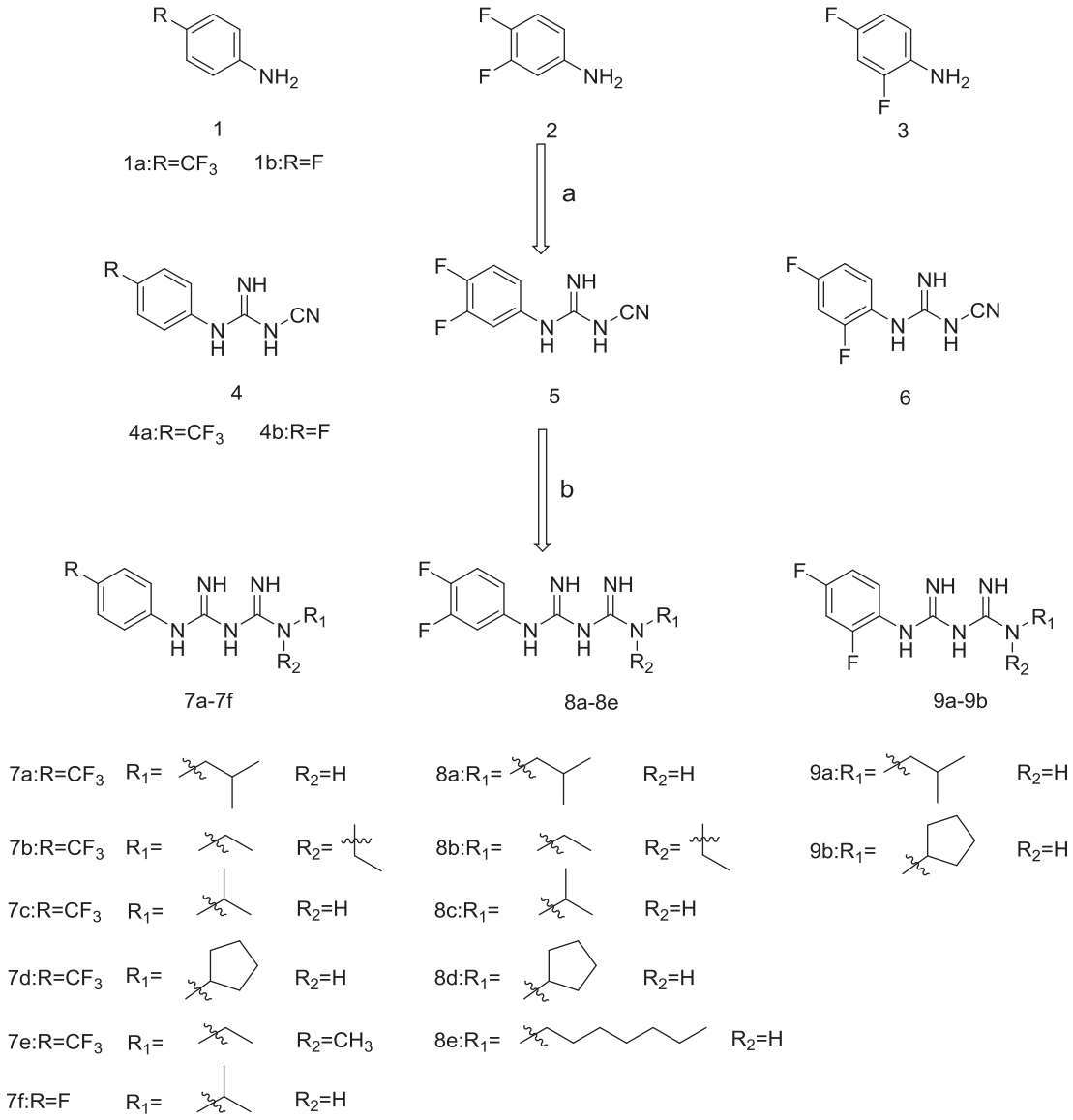

Scheme 1. Synthesis of derivatives **7a-7f, 8a-8e, 9a-9b.** Reagents and conditions: (a) NaN (CN) $_2$, HCl, 80 °C, 1h. (b) THF, $CuSO_4{\cdot}5H_2O$, alkylamines or cycloalkylamines, HCl, EDTA, 40 °C.

Table 1
The anti-proliferative activities of proguanil and its derivatives **7a-f**, **8a-e**, **9a-b** against five human cancer cell lines.

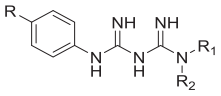
7a-7f

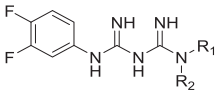
8a-8e

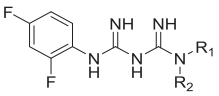
9a-9b

Compounds	R	R_1	R_2	IC_{50}(μM) ± SD				
				UMUC3	T24	A2780	A549	HCT116
proguanil				16.3 ± 1.3	18.4 ± 1.2	13 ± 1.6	3.8 ± 0.66	8.4 ± 0.98
7a	CF_3		H	2.0 ± 0.45	3.1 ± 0.38	2.1 ± 0.55	1.3 ± 0.21	3.5 ± 0.29
7b	CF_3			4.9 ± 0.86	6.2 ± 0.54	3.8 ± 0.29	3.7 ± 0.31	4.3 ± 0.45
7c	CF_3		H	5.2 ± 0.96	4.8 ± 0.77	3.2 ± 0.31	3.6 ± 0.55	4.8 ± 0.78
7d	CF_3		H	3.3 ± 0.21	3.7 ± 0.62	2.5 ± 0.26	1.8 ± 0.33	3.8 ± 0.35
7e	CF_3		CH3	6.9 ± 0.92	5.7 ± 0.48	5.1 ± 0.83	4.1 ± 0.81	4.0 ± 0.41
7f	F		H	> 50	> 50	28 ± 3.6	7.5 ± 1.3	> 50
8a			H	7.1 ± 0.45	42.9 ± 4.9	6.7 ± 0.83	2.4 ± 0.53	29.7 ± 2.5
8b				22.1 ± 1.7	44.8 ± 2.2	20.4 ± 2.8	7.8 ± 1.1	39.4 ± 2.9
8c			H	25.0 ± 2.5	45.0 ± 4.2	26 ± 3.2	5.2 ± 0.49	> 50
8d			H	7.2 ± 1.1	24.9 ± 1.7	9.3 ± 1.2	3.5 ± 0.38	16.8 ± 0.53
8e			H	2.1 ± 0.37	4.3 ± 0.35	1.5 ± 0.37	1.5 ± 0.17	1.8 ± 0.24
9a			H	17.3 ± 2.3	40.8 ± 4.3	19.8 ± 1.3	3.6 ± 0.41	21.1 ± 2.1
9b			H	18.4 ± 1.7	37.8 ± 2.9	14.7 ± 1.1	4.0 ± 0.44	29.5 ± 2.9

[a]Cell lines were treated with derivatives for 72 h.
[b]IC_{50} values are the mean of triplicate measurements.

derivative **8e** with an IC_{50} value of 1.5 μM for A2780, 1.8 μM for HCT116 was stronger than derivative **7a** (Table 1), indicating existence of cellular specificities of these derivatives. The detailed information and mechanisms of these cellular specificities, this is, why and how different derivatives have different activities in different cell lines warrant further study. However, we would like to highlight several observations to discuss preliminary structure activity relationship (SAR). For substituents on phenyl ring, derivatives with trifluoromethylphenyl substitutions (**7a**, **7c**, **7d**) showed obviously stronger activity than those with 3,4-difluorophenyl substitutions (**8a**, **8c**, **8d**), 2,4-difluorophenyl substitutions (**9a**, **9b**) or 4-fluorophenyl substitution (**7f**) targeting all tested cell lines. For R_1 substituent, when the phenyl ring was replaced with 4-trifluoromethy, the activity of derivative with R_1 of isobutyl displayed some better than that with R_1 of cyclopentyl (**7a** Vs **7d**); when the phenyl ring was substituted with 3,4-difluoro, derivative **8e** (R1 = heptyl) inhibited the best activity among four compounds of **8a**, **8c**-**8d**, it looked like the longer the alkyl chain, the higher the activity; while when the phenyl ring was 2,4-difluorophenyl, these two compounds **9a** (R_1 = isobutyl) and **9d** (R_1 = cyclopentyl) performed almost equal activity. For the replacement of R_1 and R_2 happened simultaneously, (**7b**, **7e**) Vs (**7a**, **7d**), the activity decreased dramatically to some extent. From the results obtained above, derivatives with trifluoromethylphenyl or R_1 of heptyl may make a positive contribution to anti-proliferative activity improvement. Subsequent experiments revealed that the cytotoxicity of derivatives **7a**, **7d**, and **8e** on normal cell line HUVEC was significantly lower than these cancer cell lines (Table 1, Table 2 and Fig.2), suggesting that derivatives **7a** and **8e** could be further developed as novel biguanide candidates for treating cancer.

2.3. Derivatives 7a, 7d and 8e inhibit colony formation in five cancer cell lines

Due to the excellent inhibitory activity of derivatives **7a**, **7d** and **8e** on 5 kinds of cancer cell lines in proliferation assay, their abilities to inhibit cellular colony formation were evaluated through standard colony formation assay (Fig. 3). The results showed that derivatives **7a**, **7d** and **8e** had more effective inhibition to all cell lines than proguanil. When 2 μM derivatives **7a**, **7d** and **8e** were applied, colony forming ability of four cancer cell lines (UMUC3, T24, A2780, HCT116) was dramatically inhibited, much lower than proguanil. The more interesting was that colony formation of A549 was totally inhibited at this concentration, implying that these derivatives may be more suitable for treating lung cancer. Consistent with MTT assay, derivative **7a** showed highest activity in bladder (UMUC3, T24) and lung (A549) cancer cell lines, while ovarian(A2780) and colorectal (HCT116) cancer cell lines were most sensitive to derivative **8e**.

2.4. Derivatives 7a,7d and 8e inhibit cell migration in three cancer cell lines

The effects of derivatives (**7a**, **7d** and **8e**) and proguanil on the migration of cancer cells were determined by cellular scratch assay. As shown in Fig.4, after treatment with different concentrations of derivatives **7a**,**7d** and **8e**, cell migration was significantly inhibited at 24 h and 48 h compared with the control group. In contrast, proguanil treatment at this concentration did not cause significant change. These results demonstrated that derivatives **7a**,**7d** and **8e** have stronger inhibitory effect than proguanil on migration.

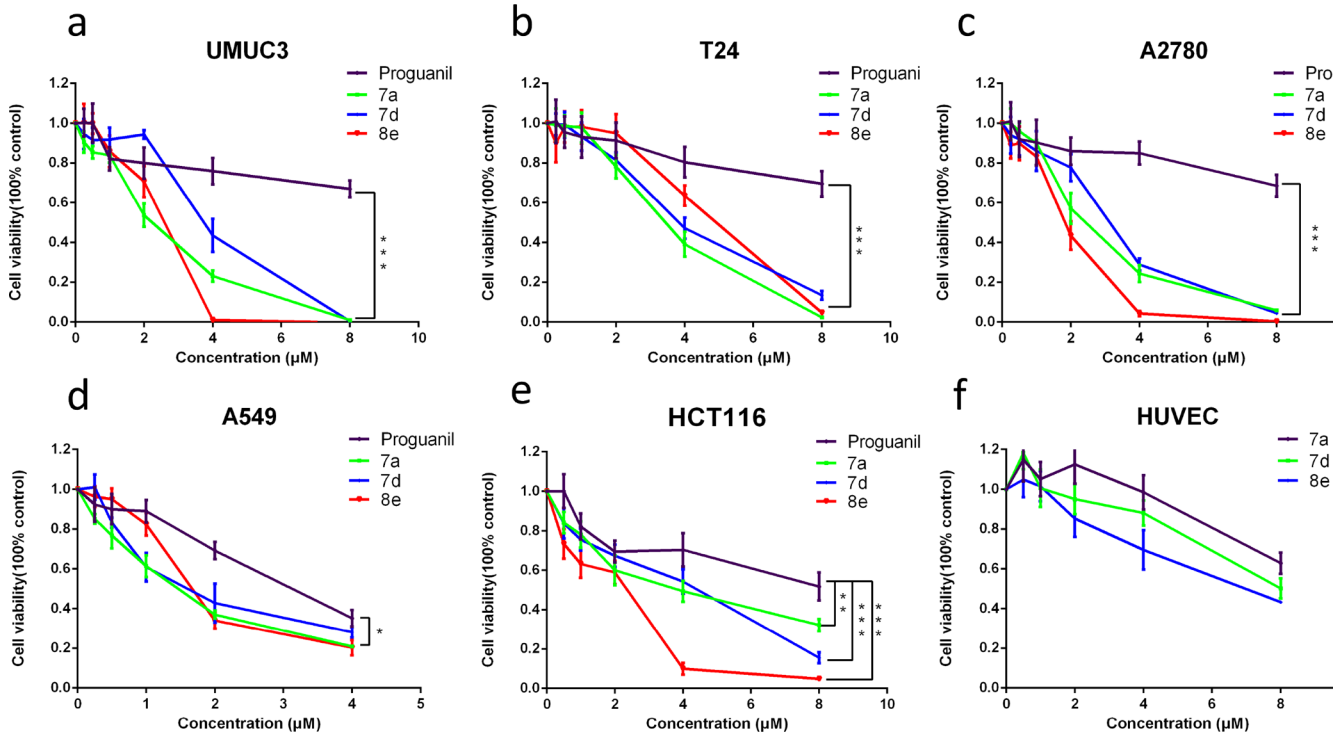

Fig. 2. Concentration-response curves for proguanil, derivatives **7a,7d** and **8e.** UMUC3, T24, A2780, HCT116 cell lines were treated with these Compounds (0–8 μM) for 72 h. A549 cell line was treated with these Compounds (0–4 μM) for 72 h. HUVEC cell line was treated with **7a,7d** and **8e** (0–8 μM) for 72 h. The results were showed as the average of 3 independent experiments (*P < 0.05, **P < 0.01, ***P < 0.001).

Table 2
The anti-proliferative activities of derivatives **7a**, **7d** and **8e** against normal cell line HUVEC.

Compounds	IC_{50}(μM) ± SD
	HUVEC
7a	8.5 ± 0.56
7d	7.3 ± 0.68
8e	6.4 ± 0.63

2.5. Derivative 7a regulates AMPK and its downstream signaling pathway

Studies have shown that AMPK as an energy regulator counts a great deal for cell proliferation.[19,20] Previously, our laboratory demonstrated that biguanides exerted anti-tumor effects mainly through the AMPK signal pathway.[21–24] For further understanding the mechanism of anti-proliferative activities of these newly synthesized derivatives, we explored the effect of derivative **7a** on AMPK signal transduction pathway. As shown in Fig.5, phosphorylation of AMPK was significantly up-regulated with concentration gradient (0–2 μM) or time gradient (0–12 h) after treatment with derivative **7a**, indicating that derivative **7a** induced activation of AMPK. Studies have shown that activation of mTOR, one of the downstream targets of AMPK,[25,26] can phosphorylate its downstream p70S6K and 4EBP1, which both played a key role in protein synthesis in cancer cells. These two downstream proteins produce translational proteins required for cells growth, which closely related with cancer progression.[27,28] Thus, we further investigated the effects of derivative **7a** on mTOR, p70S6K and 4EBP1.In Fig 5, we can see that the phosphorylation of mTOR, 4EBP1 and p70S6K were decreased in derivative **7a** treatment group. Further, we found that derivative **7a** regulated p-AMPK, p-mTOR, p-p70S6K, and p-4EBP1 much more strongly than proguanil at a concentration of 2 μM (Fig.5**i**). However, there was no significant difference in the regulatory effect of proguanil treatment group on p-AMPK compared with 0 μM treatment group, which was consistent with the results of Bridges et al. [29] This means that fluorine-containing derivatives may enhance permeability into mitochondria. These results indicated that derivative **7a** strongly activated AMPK and down-regulated the mTOR signal pathway, thereby inhibiting p70S6K and 4EBP1 phosphorylation to block the tumor cell growth (Fig.6).

3. Conclusions

In summary, we have designed and synthesized a series of proguanil derivatives by introducing trifluoromethyl and fluorine atoms into the benzene ring to discover promising anti-cancer drug candidates. The inhibitory effect of most derivatives of these newly synthesized compounds on the proliferation and migration of cancer cells is more profound than proguanil. Among them, derivative **7a** exhibited the highest anti-proliferative activities in bladder cancer cell lines (UMUC3 T24) and Lung cancer cell line (A549) while derivative **8e** shows the strongest activity to ovarian cancer cell line (A2780) and colorectal carcinoma cell line (HCT116). To further explore the anti-tumor mechanism of derivatives, western blot test showed that the derivative **7a** inhibits tumor proliferation and influencing AMPK-mTOR signal pathway. Overall, derivatives **7a** and **8e** are worthy of further study as new potential anti-proliferative drugs.

4. Experimental

4.1. Chemistry

All solvents and materials were commercial grade and no further purification was required unless otherwise stated. Infrared spectra were recorded by the Thermo Nicolet iS5 spectrometer. Proton nuclear magnetic resonance (^{1}H-NMR) spectra and ^{13}C NMR were recorded on a Brucker DRX spectrometer (600 MHz) in dimethylsulfoxide (DMSO) solvent by using TMS as an internal standard. High resolution mass spectrometry (HRMS) analysis was performed on an Agilent 1290

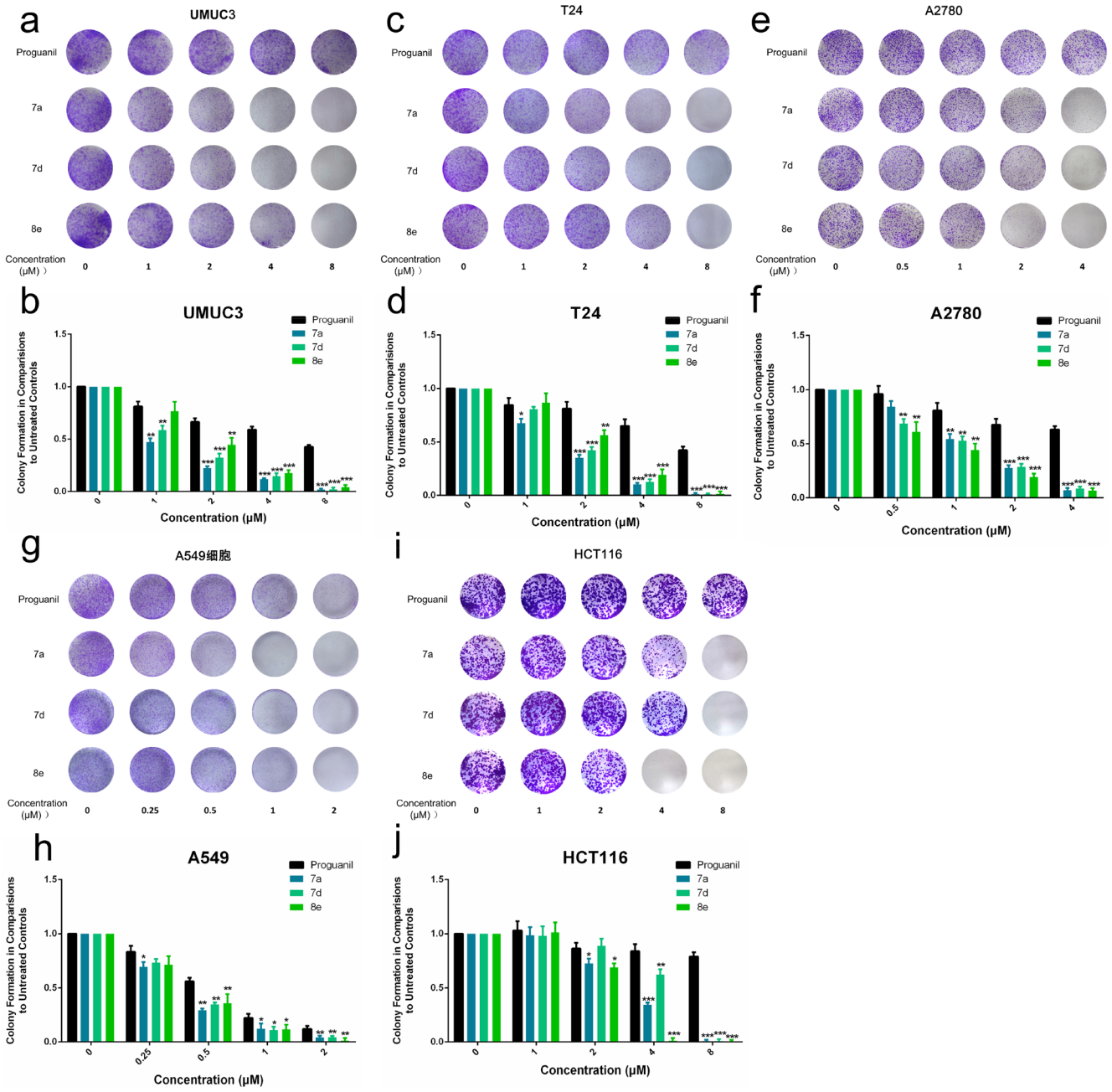

Fig. 3. Inhibitory effect of derivatives **7a, 7d** and **8e** on colony suppression to five human cancer cell lines, comparing to proguanil. (a, c, e, g and i) UMUC3, T24 and HCT116 cell lines were treated with 0–8 μM of proguanil or derivatives **7a**, **7d** and **8e**; A2780 cell line was treated with these compounds at a concentration of 0–4 μM. A549 cell line was treated with these compounds at a concentration of 0–2 μM. After7 days, the quantity of colonies was examined by counting after staining with crystal violet. (b, d, f, h and j) Bar charts showed the average quantitative data of 3 independent experiments (*P < 0.05, **P < 0.01, ***P < 0.001). Quantitative data were measured by microplate area scan (OD = 550 nm). The results were showed as the average of 3 independent experiments. (For interpretation of the references to colour in this figure legend, the reader is referred to the web version of this article.)

HPLC-6540-Q-TOF instrument. Low resolution mass spectra were acquired with an Accurate-Mass-Q-TOF MS 6520 system (Agilent Technologies, Milford, MA) equipped with an electrospray ionization (ESI) source. The melting point of the derivatives was obtained by a micro melting point apparatus XT3A. Column chromatographic separations were carried out with silica gel (200–300 mesh), and the samples were eluted with a 1:4 Petroleum ether/ethyl acetate mixture, Fractions were monitored by TLC (Qingdao Marine Chemical Inc., P. R. China) and spots were visualized by using a UV lamp. The purity of the derivatives was determined by high-performance liquid chromatography (HPLC), conducted on an agilent 1260 HPLC system with a TC-C18 column (4.6 mm × 250 mm, 5 μm), and the samples were eluted with a 45:55 methanol/H_2O mixture, at a flow rate of 1 ml/min.

*4.1.1. Method for synthesizing compounds **4,5** and **6***

NaN (CN) $_2$ (50 g, 0.56 mol) was dissolved in 430 ml of water to form a solution, and substituted anilines solution (45 g, 0.3 mol of substituted anilines dissolved in water and concentrated HCl (132 ml / 23.5 ml)) was added at 80 °C, and then maintaining the reaction at 80 °C for about 1 h. TLC detected the reaction solution until no substituted anilines was present. Finally, the white powdery solids were filtered and dried in vacuum to obtain intermediate products.

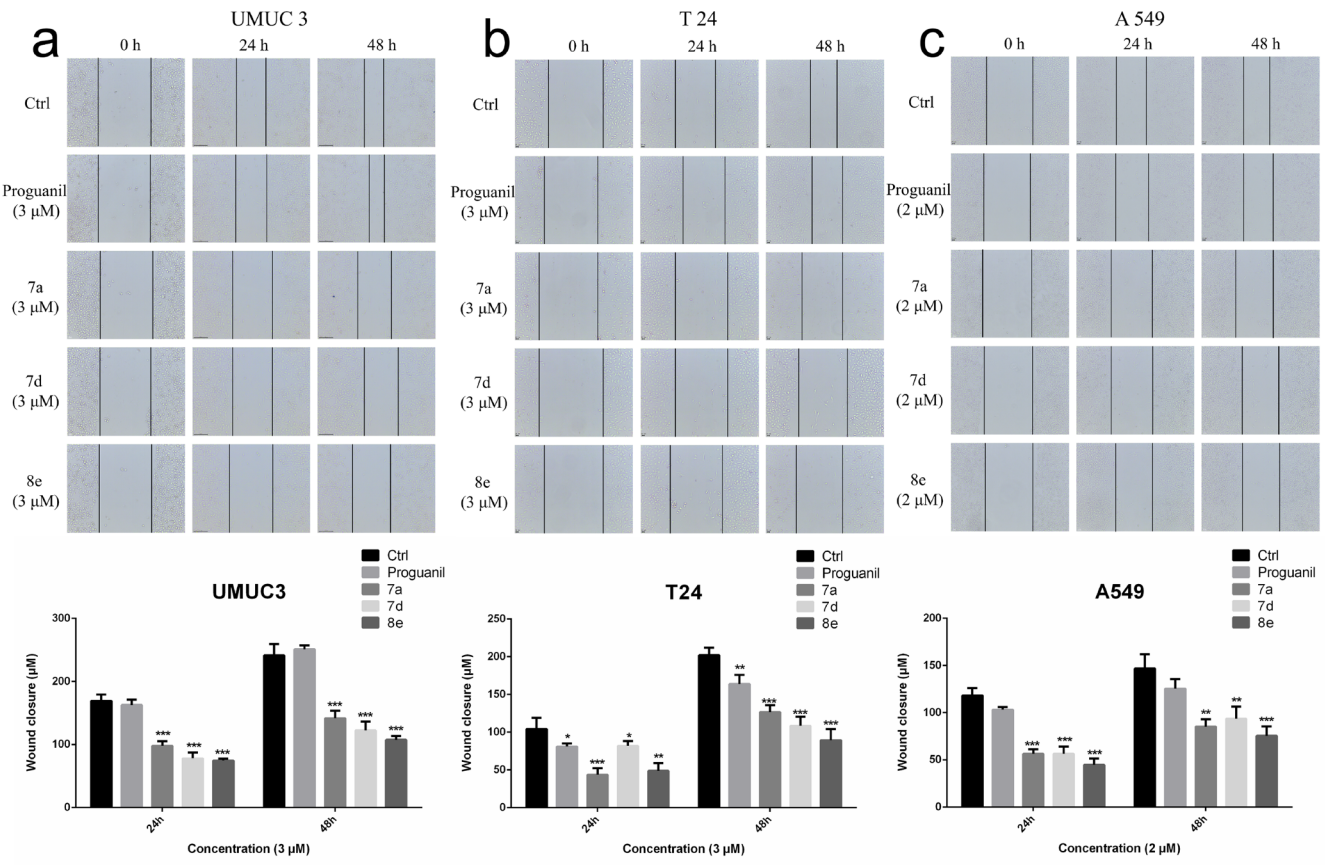

Fig. 4. Inhibitory effect of derivatives **7a, 7d** and **8e** on migration to three human cancer cell lines, comparing to proguanil. UMUC3, T24 cell lines were treated with 3 μM proguanil or derivative**7a**, **7d** and **8e**. A549 cell line was treated with these compounds at a concentration of 2 μM. (a-c) showed the gap of scratch areas and bar graphs of each cell line after drug treatment or without drug treatment (Ctrl) for 24 h or 48 h. The average wound closure distance was obtained by Image J software. The results were showed as the average of 3 independent experiments (*P < 0.05, **P < 0.01, ***P < 0.001).

4.1.1.1. 1-(4-trifluoromethyl) phenyl-3-cyanoguanidine (4a). Yield: 95.5%. ^{1}H NMR (600 MHz, DMSO-d_6) δ 9.45 (s, 1H), 7.66 (d, J = 8.5 Hz, 2H), 7.60 (d, J = 8.5 Hz, 2H). ESI-MS: m/z 229.0[M + 1]$^+$.

4.1.1.2. 1-(4-fluoro) phenyl-3-cyanoguanidine (4b). Yield: 90.7%. ^{1}H NMR (600 MHz, DMSO-d_6) δ 9.02 (s, 1H), 7.37–7.32 (m, 2H), 7.17–7.12 (m, 2H). ESI-MS: m/z176.8[M-1]$^-$.

4.1.1.3. 1-(3,4-difluoro) phenyl-3-cyanoguanidine (5). Yield: 95.2%. ^{1}H NMR (600 MHz, DMSO-d_6) δ 7.50 (d, J = 7.5 Hz, 1H), 7.34 (dd, J = 18.0, 8.9 Hz, 1H), 7.09 (d, J = 5.8 Hz, 1H). ESI-MS: m/z197.0[M + 1]$^+$.

4.1.1.4. 1-(2,4-difluoro) phenyl-3-cyanoguanidine (6). Yield: 94.9%.^{1}H NMR (600 MHz, DMSO-d_6) δ 8.87 (s, 1H), 7.59 (d, J = 6.2 Hz, 1H), 7.35–7.29 (m, 1H), 7.07 (d, J = 8.6 Hz, 1H). ESI-MS: m/z194.8[M-1]$^-$.

4.1.2. Method for synthesizing derivatives 7a-7e

9.12 g (0.04 mol) of 1-(4-trifluoromethyl) phenyl-3-cyanoguanidine was added to 48 ml of THF and 40 ml of water while stirring at 25–35 °C, followed by addition of 6.8 g (0.085 mol) of copper sulfate pentahydrate and 0.16 mol of alkylamines or cycloalkylamines. The mixed solution was heated to 40 °C and continuously stirred. After the TLC was used to check the absence of 1-(4-trifluoromethyl) phenyl-3-cyanoguanidine, the THF was evaporated to dryness under reduced pressure. When the products was cooled to 25–30 °C, HCl solution (20 ml of concentrated hydrochloric acid in 32 ml of water) was added and stirred for 30 min, and cooled ammonia EDTA solution (32 ml of water, 15 ml of ammonia water (25%) and 14 g EDTA disodium disodium salt) was dropped to the reactive mixture, maintaining the temperature in the range of 15–20 °C. After that, the mixture was stirred at the same temperature for 30 min. The products were separated by filtration and repeatedly washed in cold water, and then dried at 90–95 °C. Finally, derivatives were purified by column chromatography on silica gel.

4.1.2.1. 1-isobutyl-5-(4-trifluoromethylphenyl) biguanide(7a). Yield: 56.9%. Mp: 213–215 °C. IR: n/cm^{-1}: 3306, 3155 (NH), 1634(C═N). ^{1}H NMR (600 MHz, DMSO) δ 10.22 (s, 1H), 7.65 (d, J = 13.6 Hz, 2H), 7.62 (d, J = 9.4 Hz, 2H), 2.93 (d, J = 31.9 Hz, 2H), 1.31–1.19 (m, 1H), 0.89 (d, J = 6.2 Hz, 6H). ^{13}C NMR (151 MHz, Methanol-d_4) δ 160.04, 153 99, 142.19, 126.98, 125.02, 123.65, 119.95, 53.61, 32.36, 23.28. ESI-MS: m/z 302.1[M + 1]$^+$. HRMS (ESI) (m/z) [M + H]$^+$ calcd for $C_{13}H_{18}F_3N_5$, 302.1548; found, 302.1594. Purity: 99.9% (by HPLC).

4.1.2.2. 1-diethyl-5-(4-trifluoromethylphenyl) biguanide(7b). Yield: 39.5%. Mp: 215–217 °C. IR: n/cm^{-1}: 3310, 3162 (NH), 1637(C═N). ^{1}H NMR (600 MHz, DMSO-d_6) δ 9.93 (s, 1H), 7.72 (s, 2H), 7.65 (d, J = 8.7 Hz, 2H), 7.60 (d, J = 8.7 Hz, 2H), 3.40–3.34 (m, 4H), 1.18–1.04 (m, 6H). ^{13}C NMR (151 MHz, Methanol-d_4) δ 159.39, 153.99, 142.49, 126.98, 125.52, 123.65, 119.95, 42.80, 11.78. ESI-MS: m/z302.1[M + 1]$^+$. HRMS (ESI) (m/z) [M + H]$^+$ calcd for $C_{13}H_{18}F_3N_5$, 302.1548; found, 302.1605.

4.1.2.3. 1-isopropyl-5-(4-trifluoromethylphenyl) biguanide(7c). Yield:46.3%. ^{1}H NMR (600 MHz, DMSO-d_6) δ 7.51 (d, J = 8.2 Hz, 3H), 7.16–7.00 (m, 2H), 3.85 (s, 1H), 1.10 (d, J = 6.4 Hz, 6H). ^{13}C NMR (151 MHz, Methanol-d_4) δ 158.93, 156.33, 147.56, 127.36, 125.32, 123.65, 121.61,

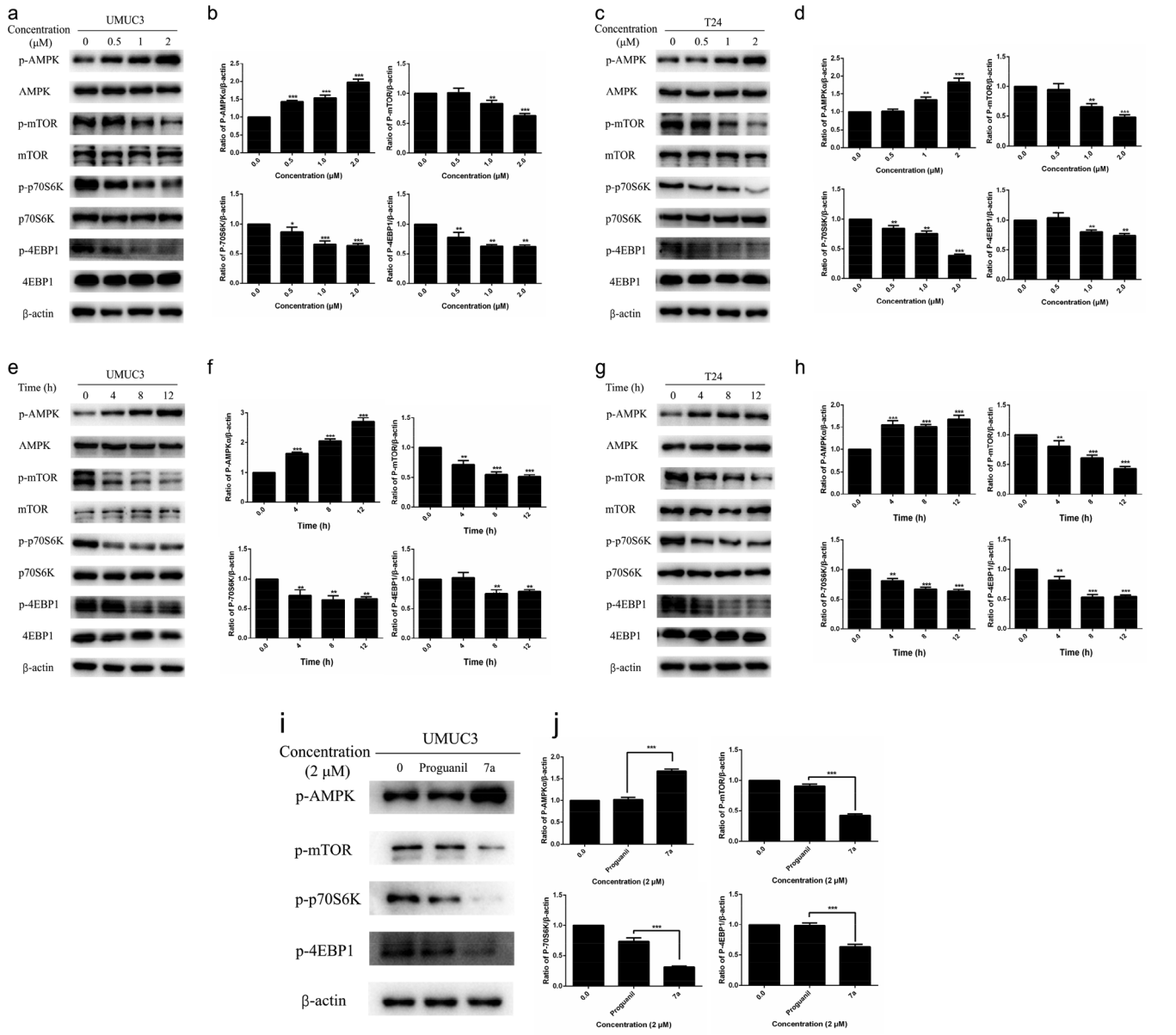

Fig. 5. Effect of derivative **7a** on the expression of AMPK and its downstream pathway in UMUC3 and T24 Cells. (a and c) Effect of derivative **7a** in protein levels (p-AMPK, p-mTOR, p-p70S6K, p-4EBP1, *t*-AMPK, *t*-mTOR, t-p70S6K and t-4EBP1) of bladder cancer cell lines treated with derivative **7a** for 12 h. (e and g) Effect of derivative **7a** in protein levels (p-AMPK, p-mTOR, p-p70S6K, p-4EBP1, *t*-AMPK, *t*-mTOR, t-p70S6K and t-4EBP1) of bladder cancer cell lines treated with derivative **7a** at a concentration of 2 μM. (i) Effect of derivative **7a** and proguanil in protein levels (p-AMPK, p-mTOR, p-p70S6K, p-4EBP1) of UMUC3 treated with compounds at a concentration of 2 μM. Equal loading was established by β-actin. The density values of each protein were obtained by imagine J software, (b, d, f, h and j) show the ratio of optical density values of these proteins to β-actin. Results were expressed as the mean of 3 independent experiments (*P < 0.05, **P < 0.01, ***P < 0.001).

43.10, 20.94. HRMS (ESI) (*m/z*) $[M+H]^+$ calcd for $C_{12}H_{16}F_3N_5$, 288.1391; found, 288.1444.

4.1.2.4. 1-cyclopentyl-5-(4-trifluoromethylphenyl) biguanide(7d). Yield: 51.7%. Mp:225–227 °C. IR: n/cm^{-1}: 3307,3186 (NH), 1626(C═N). ^1H NMR (600 MHz, DMSO) δ 9.54 (s, 1H), 8.19 (s, 1H), 7.64 (d, J = 4.1 Hz, 2H), 7.58 (d, J = 7.5 Hz, 2H), 3.93–3.72 (m, 1H), 1.96–1.60 (m, 4H), 1.56–1.40 (m, 4H). ESI-MS: *m/z* 314.1[M+1] $^+$. ^{13}C NMR (151 MHz, Methanol-d_4) δ 160.34, 154.59, 142.81, 126.98, 125.32, 123.28, 120.25, 53.61, 32.36, 23.28. HRMS (ESI) (*m/z*) [M+H] $^+$ calcd for $C_{14}H_{18}F_3N_5$, 314.1548; found, 314.1603. Purity: 96.6% (by HPLC).

4.1.2.5. 1-methyl-1-ethyl-5-(4-trifluoromethylphenyl) biguanide(7e). Yield: 59.2%. Mp: 201–203 °C. IR: n/cm^{-1}: 3362 (NH), 1649(C═N). ^1H NMR (600 MHz, DMSO-d_6) δ 9.81 (s, 1H), 7.74 (s, 2H), 7.65 (d, J = 8.0 Hz, 2H), 7.61 (d, J = 7.6 Hz, 2H), 3.37 (q, J = 7.0 Hz, 2H), 2.97 (s, 3H), 1.18–0.96 (m, 3H). ^{13}C NMR (151 MHz, Methanol-d_4) δ 160.04, 153.31, 142.19, 126.98, 125.62, 123.65, 119.57, 45.52, 33.72, 11.10. ESI-MS: *m/z* 288.0[M+1] $^+$. HRMS (ESI) (*m/z*) [M+H] $^+$ calcd for $C_{12}H_{16}F_3N_5$, 288.1396; found, 288.1450.

4.1.3. Method for synthesizing derivatives 7f

7.12 g (0.04 mol) of 1-(4-fluoro) phenyl-3-cyanoguanidine was added to 48 ml of THF and 40 ml of water while stirring at 25–35 °C,

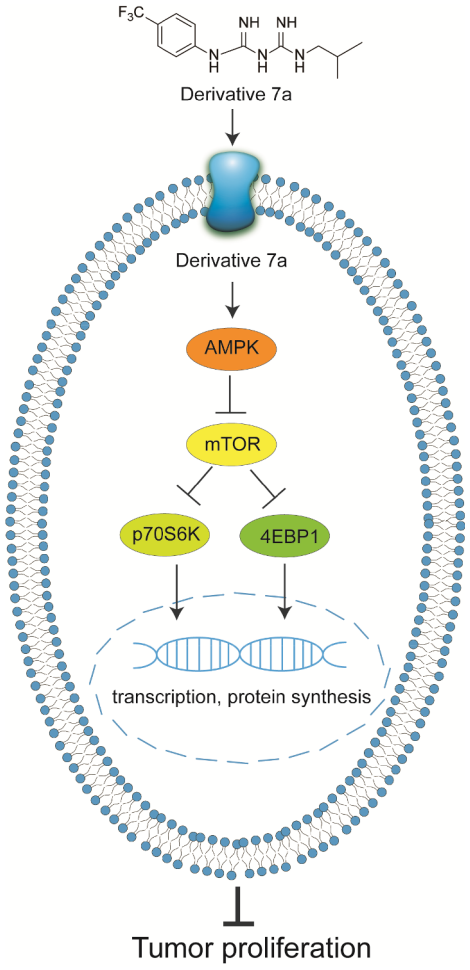

Fig. 6. Schematic diagram of derivative 7a on AMPK cell signaling pathway.

followed by addition of 6.8 g (0.085 mol) of copper sulfate pentahydrate and 0.16 mol of isopropylamine. The mixed solution was heated to 40 °C and continuously stirred. After the TLC was used to check the absence of 1-(4-fluoro) phenyl-3-cyanoguanidine, the THF was evaporated to dryness under reduced pressure. When the products was cooled to 25–30 °C, HCl solution (20 ml of concentrated hydrochloric acid in 32 ml of water) was added and stirred for 30 min, and cooled ammonia EDTA solution (32 ml of water, 15 ml of ammonia water (25%) and 14 g EDTA disodium disodium salt) was dropped to the reactive mixture, maintaining the temperature in the range of 15–20 °C. After that, the mixture was stirred at the same temperature for 30 min. The products were separated by filtration and repeatedly washed in cold water, and then dried at 90-95℃. Finally, derivatives were purified by column chromatography on silica gel.

4.1.3.1. 1-isopropyl-5-(4-fluorophenyl) biguanide (7f). Yield:49.5%. 1H NMR (600 MHz, DMSO-d_6) δ 9.85 (s, 1H), 9.54 (s, 1H), 7.44–7.33 (m, 2H), 7.18–7.12 (m, 2H), 3.69 (s, 1H), 1.11 (d, J = 6.5 Hz, 6H). ^{13}C NMR (151 MHz, Methanol-d_4) δ 160.34, 158.68, 133.71, 123.96, 115.18, 43.48, 21.24. HRMS (ESI) (m/z) $[M+H]^+$ calcd for $C_{11}H_{16}FN_5$, 238.1423; found, 238.1485. Purity: 99.4% (by HPLC).

4.1.4. Method for synthesizing derivatives 8a-8e

7.84 g (0.04 mol) of 1-(3,4-difluoro) phenyl-3-cyanoguanidine was added to 48 ml of THF and 40 ml of water while stirring at 25–35 °C, followed by addition of 6.8 g (0.085 mol) of copper sulfate pentahydrate and 0.16 mol of alkylamines or cycloalkylamines. The mixed solution was heated to 40 °C and continuously stirred. After the TLC was used to check the absence of 1-(3,4-difluoro) phenyl-3-cyanoguanidine, the THF was evaporated to dryness under reduced pressure. When the products was cooled to 25–30 °C, HCl solution (20 ml of concentrated hydrochloric acid in 32 ml of water) was added and stirred for 30 min, and cooled ammonia EDTA solution (32 ml of water, 15 ml of ammonia water (25%) and 14 g EDTA disodium disodium salt) was dropped to the reactive mixture, maintaining the temperature in the range of 15–20 °C. After that, the mixture was stirred at the same temperature for 30 min. The products were separated by filtration and repeatedly washed in cold water, and then dried at 90-95℃. Finally, derivatives were purified by column chromatography on silica gel.

4.1.4.1. 1-isobutyl-5-(3,4-difluorophenyl) biguanide(8a). Yield:65.6%. Mp:179–181 °C. IR: n/cm^{-1}: 3313 (NH), 1641(C=N). ^{1}H NMR (600 MHz, DMSO-d_6) δ 9.63 (s, 1H), 8.12 (s, 1H), 7.88–7.67 (m, 1H), 7.64–7.48 (m, 1H), 7.36 (d, J = 7.6 Hz, 1H), 3.02–2.85 (m, 2H),1.87–1.66 (m, 1H) ,0.86 (d, J = 33.4 Hz, 6H). ESI-MS: m/z 270.0$[M+1]^+$. ^{13}C NMR (151 MHz, Methanol-d_4) δ 160.72, 155.65, 154.29, 150.58, 148.54, 117.60, 116.54, 110.49, 48.85, 27.67, 18.89. HRMS (ESI) (m/z) $[M+H]^+$ calcd for $C_{12}H_{17}F_2N_5$, 270.1486; found, 270.1535.

4.1.4.2. 1,1-diethyl-5-(3,4-difluorophenyl) biguanide(8b). Yield:42.3%. Mp:178–180 °C. IR: n/cm^{-1}: 3306, 3189 (NH), 1628(C=N). ^{1}H NMR (600 MHz, DMSO-d_6) δ 9.72 (s, 1H), 7.55 (d, J = 10.2 Hz, 1H), 7.37 (dd, J = 19.2, 9.4 Hz, 1H),7.11 (d, J = 6.4 Hz, 1H), 3.41–3.33 (m, 4H), 1.28–0.98 (m, 6H). ^{13}C NMR (151 MHz, DMSO-d_6) δ 159.14, 154.02, 150.16, 148.46, 146.22, 117.84, 116.60, 109.42, 42.50, 13.50. ESI-MS: m/z 270.1$[M+1]^+$. HRMS (ESI) (m/z) $[M+H]^+$ calcd for $C_{12}H_{17}F_2N_5$, 270.1486; found, 270.1537. Purity: 99.0% (by HPLC).

4.1.4.3. 1-isopropyl-5-(3,4-difluorophenyl) biguanide(8c). Yield:46.5%. Mp:223–225 °C. IR: n/cm^{-1}: 3305, 3187 (NH), 1647(C=N). ^{1}H NMR (600 MHz, DMSO-d_6) δ 9.63 (s, 1H), 8.02 (s, 1H), 7.74 (d, J = 35.8 Hz, 1H), 7.63–7.49 (m, 1H), 7.36 (d, J = 8.1 Hz, 1H), 7.10 (d, J = 8.0 Hz, 2H), 6.75 (s, 1H), 3.86–3.58 (m, 1H), 1.12 (d, J = 6.5 Hz, 6H). ESI-MS: m/z256.1$[M+1]^+$. ^{13}C NMR (151 MHz, Methanol-d_4) δ 161.70, 159.36, 155.27, 150.89, 148.92, 117.91, 116.54, 110.87, 43.78, 20.94. HRMS (ESI) (m/z) $[M+H]^+$ calcd for $C_{11}H_{15}F_2N_5$, 256.1329; found, 256.1376.

4.1.4.4. 1-cyclopentyl-5-(3,4-difluorophenyl) biguanide(8d). Yield:71.3%. Mp:215–217 °C. IR: n/cm^{-1}: 3317 (NH), 1603(C=N). ^{1}H NMR (600 MHz, DMSO-d_6) δ 9.85 (s, 1H), 8.12 (s, 1H), 7.74 (d, J = 30.2 Hz, 1H), 7.43–7.27 (m, 1H), 7.23–7.15 (m, 1H), 3.96–3.75 (m, 1H), 1.98–1.61 (m, 4H), 1.59–1.39 (m, 4H). ESI-MS: m/z 282.1$[M+1]^+$. ^{13}C NMR (151 MHz, Methanol-d_4) δ 160.34, 155.95, 153.61, 150.58, 148.92, 117.60, 116.75, 140.74, 53.23, 32.05, 22.90. HRMS (ESI) (m/z) $[M+H]^+$ calcd for $C_{13}H_{17}F_2N_5$, 282.1486; found, 282.1538. Purity: 98.3% (by HPLC).

4.1.4.5. 1-n-heptyl-5-(3,4-difluorophenyl) biguanide(8e). Yield:60.3%. Mp:119–121 °C. IR: n/cm^{-1}: 3308, 3192 (NH), 1644(C=N). ^{1}H NMR (600 MHz, DMSO-d_6) δ 9.98–9.78 (m, 1H), 8.09 (s, 1H), 7.74 (d, J = 22.0 Hz, 1H), 7.42–7.32 (m, 1H), 7.10 (d, J = 8.9 Hz, 1H), 3.14–3.05 (m, 2H), 1.58–1.37 (m, 2H), 1.33–1.16 (m, 8H), 0.90–0.81 (m, 3H). ^{13}C NMR (151 MHz, DMSO-d_6) δ 161.02, 154.97, 153.81, 150.28, 148.24, 117.91, 116.83, 109.51, 42.11, 31.68, 29.63, 28.65, 26.61, 22.90, 13.82. ESI-MS: m/z 309.9$[M-1]^-$. HRMS (ESI) (m/z) $[M+H]^+$ calcd for $C_{15}H_{23}F_2N_5$, 312.1955; found, 312.2008.

4.1.5. Method for synthesizing derivatives 9a-9b

7.84 g (0.04 mol) of 1-(2,4-difluoro) phenyl-3-cyanoguanidine was added to 48 ml of THF and 40 ml of water while stirring at 25–35 °C, followed by addition of 6.8 g (0.085 mol) of copper sulfate pentahydrate and 0.16 mol of alkylamines or cycloalkylamines. The mixed

solution was heated to 40 °C and continuously stirred. After the TLC was used to check the absence of 1-(2,4-difluoro) phenyl-3-cyanoguanidine, the THF was evaporated to dryness under reduced pressure. When the products was cooled to 25–30 °C, HCl solution (20 ml of concentrated hydrochloric acid in 32 ml of water) was added and stirred for 30 min, and cooled ammonia EDTA solution (32 ml of water, 15 ml of ammonia water (25%) and 14 g EDTA disodium disodium salt) was dropped to the reactive mixture, maintaining the temperature in the range of 15–20 °C. After that, the mixture was stirred at the same temperature for 30 min. The products were separated by filtration and repeatedly washed in cold water, and then dried at 90-95℃. Finally, derivatives were purified by column chromatography on silica gel.

4.1.5.1. 1-isobutyl-5-(2,4-difluorophenyl) biguanide(9a). Yield:54.8%. Mp:189–181 °C. IR: n/cm^{-1}: 3305, 3192 (NH), 1604(C=N). ^1H NMR (600 MHz, DMSO-d_6) δ 9.09 (s, 1H), 7.89 (s, 1H), 7.29 (d, J = 17.6 Hz, 1H), 7.11–7.03 (m, 1H), 6.97 (d, J = 20.3 Hz, 1H), 2.92 (d, J = 17.0 Hz, 2H), 1.83–1.61 (m, 1H), 0.87 (d, J = 19.6 Hz, 6H). ESI-MS: m/z 267.9[M-1]$^-$. ^{13}C NMR (151 MHz, Methanol-d_4) δ 161.40 160.72 156.63 154.97 127.36 122.29 110.49 103.76 48.85 28.35 18.89. HRMS (ESI) (m/z) $[M+H]^+$ calcd for $C_{12}H_{17}F_2N_5$, 270.1486; found, 270.1529.

4.1.5.2. 1-cyclopentyl-5-(2,4-difluorophenyl) biguanide(9b). Yield:81.2%. Mp:217–219 °C. IR: n/cm^{-1}: 3360 (NH), 1603(C=N). ^1H NMR (600 MHz, DMSO-d_6) δ 8.79 (s, 1H), 8.10–7.93 (m, 1H), 7.65 (s, 2H), 7.31 (t, J = 8.7 Hz, 1H), 7.10–7.05 (m, 1H), 6.84 (s, 1H), 4.00–3.64 (m, 1H), 1.95–1.57 (m, 4H), 1.57–1.34 (m, 4H). ESI-MS: m/z 282.1$[M+1]^+$. ^{13}C NMR (151 MHz, DMSO-d_6) δ 160.10, 159.64, 156.27, 154.73, 126.98, 122.97, 111.48, 104.44, 52.93, 32.66, 23.58. HRMS (ESI) (m/z) $[M+H]^+$ calcd for $C_{13}H_{17}F_2N_5$, 282.1486; found, 282.1533. Purity: 98.9% (by HPLC).

4.2. Cell lines and culture conditions

Two human bladder cancer cell lines (T24, UMUC3) were obtained from Dr. P Guo (Xi'an Jiaotong University, China). Human ovarian cancer cell line (A2780) was a gift from Dr. Y Zhang (Xiangya Hospital, China). Human lung cancer cell line (A549) and colorectal cancer cell line (HCT116) were purchased from ATCC. All cells were grown in DMEM (Hyclone, Logan, UT, USA) or RPMI-1640 (Hyclone, Logan, UT, USA) supplied with 10% FBS (Hyclone, Logan, UT, USA) and 1% penicillin/streptomycin mixture. Besides, cells were maintained in a 37 ℃, 5% CO_2 humidified incubator.

4.3. Cell viability assay

The effect of the compounds on the viability of human bladder cancer cell lines (T24, UMUC3), human lung cancer cell line(A549), and human ovarian cancer cell line(A2780) were determined by MTT assay. Several cell lines(6.0 × 103 cells per well) were plated in 96-well plates. After 12 h, cells were treated with different concentrations of compounds in triplicate for 72 h. Then MTT solution(2 mg/mL, 50 μL) was transferred into each well to replace the medium and incubated for 6 h at 37 °C. Finally, 150 μL DMSO was added to each well and the optical density was measured at 490 nm by using a microplate reader (Biotek, SYNERGY HTX, Vermont, USA).

4.4. Clonogenic assay

Several cell lines (8.0×10^3 cells per well) were plated in 24-well plates. After 24 h, cells were treated with different concentrations of compounds in triplicate for 6–8 days. After washing with phosphate-buffered saline (PBS), the cells were fixed with 10% formaldehyde solution. Finally, 0.1% crystal violet is added to each well to stain the cells. Absorbance was measured at 490 nm by using a microplate reader (Biotek)

4.5. Measurement of cell migration

Several cell lines (3.0 × 103 cells per well) were plated in 12-well plates and allowed to reach confluence. Then use a 10 μL sterile pipette tip to scratch a straight line at the center of the plate. After washing twice with PBS, serum-free medium in which compounds were dissolved was added to each well. Finally, photographs were taken at 0, 24, and 48 h using a DFC450C microscope (Leica). The experiments were repeated three times.

4.6. Protein characterization

Protein extracts of cells were loaded and run on 8% or 10% sodium dodecyl sulphate polyacrylamide gel electrophoresis (SDS-PAGE). Later, proteins were transferred onto polyvinylidene fluoride (PVDF) membranes and blocked in 5% milk in TBST for 1 h. the membranes were blotted with the specific primary antibodies at 4 °C overnight, then washed three times with Tris-buffered saline with 0.1% Tween (TBST) the next day. After incubating with secondary antibodies for 1 h, the membrane was washed three times with TBST again. Protein signals were immediately detected with a Chemi Doc (Bio-Rad, Hercules, CA, USA) after adding Pierce Super Signal chemiluminescent substrate (Rockford, IL, USA).

Acknowledgements

This study was supported by the National Natural Science Foundation of China, China (81874212); the Key Project of Hunan Province, China (2016JC2036); the Key Laboratory of Study and Discovery of Small Targeted Molecules of Hunan Province, Hunan Normal University, China (2017TP1020); Huxiang High-Level Talent Innovation Team, China (2018RS3072)

Declaration of Competing Interest

The authors declare that there are no conflicts of interests.

Appendix A. Supplementary material

Supplementary data to this article can be found online at https://doi.org/10.1016/j.bmc.2019.115258.

References

1. Freddie B, Jacques F, Isabelle S, et al. Global cancer statistics 2018: GLOBOCAN estimates of incidence and mortality worldwide for 36 cancers in 185 countries. *CA Cancer J Clin.* 2018;68(6):394–424. https://doi.org/10.3322/caac.21492.
2. Cameron A, Logie L, Patel K, et al. Metformin selectively targets redox control of complex I energy transduction. *Redox Biol.* 2017;14:187–197. https://doi.org/10.1016/j.redox.2017.08.018.
3. Deng J, Peng M, Wang Z, et al. Novel application of metformin combined with targeted drugs on anticancer treatment. *Cancer Sci.* 2019;110(1):23–30. https://doi.org/10.1111/cas.13849.
4. Barata L, Houzé P, Boutbibe K, et al. In vitro analysis of the interaction between atovaquone and proguanil against liver stage malaria parasites. *Antimicrob Agents Chemother.* 2016;60(7):4333–4335. https://doi.org/10.1128/AAC.01685-15.
5. Ma L, Wei J, Wan J, et al. Low glucose and metformin-induced apoptosis of human ovarian cancer cells is connected to ASK1 via mitochondrial and endoplasmic reticulum stress-associated pathways. *J Exp Clin Cancer Res.* 2019;38(1):77. https://doi.org/10.1186/s13046-019-1090-6.
6. Eikawa S, Nishida M, Mizukami S, et al. Immune-mediated antitumor effect by type 2 diabetes drug, metformin. *Proc Natl Acad Sci U S A.* 2015;112(6):1809–1814. https://doi.org/10.1073/pnas.1417636112.
7. Barbieri F, Würth R, Pattarozzi A, et al. Inhibition of chloride intracellular channel 1 (CLIC1) as biguanide class-effect to impair human glioblastoma stem cell viability. *Front Pharmacol.* 2018;9:899. https://doi.org/10.3389/fphar.2018.00899.
8. Lea MA, Kim H, desBORDES C. Effects of biguanides on growth and glycolysis of bladder and colon cancer cells. *Anticancer Res.* 2018;38(9):5003–5011. https://doi.org/10.21873/anticanres.12819.
9. Guan A, Liu C, Yang X, et al. Application of the Intermediate derivatization approach in agrochemical discovery. *Chem Rev.* 2014;114(14):7079–7107. https://doi.org/10.1021/cr4005605.

10. Hagmann WK. The many roles for fluorine in medicinal chemistry. *J Med Chem.* 2008;51(15):4359–4369. https://doi.org/10.1021/jm800219f.
11. Zhao Y, Guo C, Wang L, et al. A novel fluorinated thiosemicarbazone derivative- 2-(3,4-difluorobenzylidene) hydrazinecarbothioamide induces apoptosis in human A549 lung cancer cells via ROS-mediated mitochondria-dependent pathway. *Biochem Biophys Res Commun.* 2017;491(1):65–71. https://doi.org/10.1016/j.bbrc.2017.07.042.
12. Wang BC, Wang LJ, Jiang B, et al. Application of fluorine in drug design during 2010–2015 years: a mini-review. *Mini Rev Med Chem.* 2017;17(8):683–692. https://doi.org/10.2174/1389557515666151016124957.
13. Wang J, Sánchez-Roselló M, Aceña JL, et al. Fluorine in pharmaceutical industry: fluorine-containing drugs introduced to the market in the last decade (2001–2011). *Chem Rev.* 2014;114(4):2432–2506. https://doi.org/10.1021/cr4002879.
14. Li MD, Zheng YG, Ji M. Synthesis of gefitinib from methyl 3-hydroxy-4-methoxybenzoate. *Molecules.* 2007;12(3):673–678. https://doi.org/10.3390/12030673.
15. Zhou Y, Wang J, Gu Z, et al. Next generation of fluorine-containing pharmaceuticals, compounds currently in phase II-III clinical trials of major pharmaceutical companies: new structural trends and therapeutic areas. *Chem Rev.* 2016;116(2):422–518. https://doi.org/10.1021/acs.chemrev.5b00392.
16. Tao T, He C, Deng J, et al. A novel synthetic derivative of quercetin, 8-trifluoromethyl-3,5,7,3',4'–pentamethyl-quercetin, inhibits bladder cancer growth by targeting the AMPK/mTOR signaling pathway. *Oncotarget.* 2017;8(42):71657–71671. https://doi.org/10.18632/oncotarget.17799.
17. Sathe D G, Mondkar H K, Jadhav T S, et al. Process for preparation of proguanil hydrochloride[P]. WO 2009113092, 2009-09-17. doi: WO2009113092 A2.
18. Cianchetta G, Delabarre B, Popovici-muller J, et al. Aryltriazinediamine compounds as IDH2 inhibitors and their preparation and use in the treatment of cancer [P]. WO2013102431, 2013-07-11. doi: WO2013102431 A1.
19. Vazirian M, Nabavi SM, Jafari S, et al. Natural activators of adenosine 5′-monophosphate (AMP)-activated protein kinase (AMPK) and their pharmacological activities. *Food Chem Toxicol.* 2018;122:69–79. https://doi.org/10.1016/j.fct.2018.09.079.
20. Vara-Ciruelos D, Russell FM, Hardie DG. The strange case of AMPK and cancer: Dr Jekyll or Mr Hyde? *Open Biol.* 2019;9(7):190099https://doi.org/10.1098/reob.190099.
21. Peng M, Huang Y, Tao T, et al. Metformin and gefitinib cooperate to inhibit bladder cancer growth via both AMPK and EGFR pathways joining at Akt and Erk. *Sci Rep.* 2016;6:28611. https://doi.org/10.1038/srep28611.
22. Huang Y, Zhou S, He C, et al. Phenformin alone or combined with gefitinib inhibits bladder cancer via AMPK and EGFR pathways. *Cancer Commun (Lond).* 2018;38(1):50. https://doi.org/10.1186/s40880-018-0319-7.
23. Peng M, Su Q, Zeng Q, et al. High efficacy of intravesical treatment of metformin on bladder cancer in preclinical model. *Oncotarget.* 2016;7(8):9102–9117. https://doi.org/10.18632/oncotarget.6933.
24. Zhou S, Xu L, Cao M, et al. Anticancer properties of novel pyrazole-containing biguanide derivatives with activating the adenosine monophosphate-activated protein kinase signaling pathway. *Arch Pharm Chem Life Sci.* 2019;e1900075. https://doi.org/10.1002/ardp.201900075.
25. Cork GK, Thompson J, Slawson C. Real Talk: The Inter-play Between the mTOR, AMPK, and Hexosamine Biosynthetic Pathways in Cell Signaling. *Front Endocrinol (Lausanne).* 2018;9:522. https://doi.org/10.3389/fendo.2018.00522.
26. Cao C, Han D, Su Y, et al. Ginkgo biloba exocarp extracts induces autophagy in Lewis lung cancer cells involving AMPK / mTOR / p70S6k signaling pathway. *Biomed Pharmacother.* 2017;93:1128–1135. https://doi.org/10.1016/j.biopha.2017.07.036.
27. Wang XW, Zhang YJ. Targeting mTOR network in colorectal cancer therapy. *World J Gastroenterol.* 2014;20(15):4178–4188. https://doi.org/10.3748/wjg.v20.i15.4178.
28. Wei Q, Zhang B, Li P, et al. Maslinic Acid Inhibits Colon Tumorigenesis by the AMPK-mTOR Signaling Pathway. *J Agric Food Chem.* 2019;67(15):4259–4272. https://doi.org/10.1021/acs.jafc.9b00170.
29. Bridges HR, Sirviö VA, Agip AN, et al. Molecular features of biguanides required for targeting of mitochondrial respiratory complex I and activation of AMP-kinase. *BMC Biol.* 2016;14:65. https://doi.org/10.1186/s12915-016-0287-9.